

# DOSE: Detecting User-Driven Operating States of Electronic Devices from a Single Sensing Point

Ke-Yu Chen<sup>1</sup>, Sidhant Gupta<sup>2</sup>, Eric C. Larson<sup>3</sup>, Shwetak Patel<sup>1</sup>

<sup>1</sup>University Of Washington  
Seattle, WA, US  
[{kychen, shwetak}@uw.edu](mailto:{kychen, shwetak}@uw.edu)

<sup>2</sup>Microsoft Research  
Redmond, WA, US  
[sidhant@microsoft.com](mailto:sidhant@microsoft.com)

<sup>3</sup>Southern Methodist University  
Dallas, TX, US  
[eclarson@lyle.smu.edu](mailto:eclarson@lyle.smu.edu)

**Abstract**—Electricity and appliance usage information can often reveal the nature of human activities in a home. For instance, sensing the use of vacuum cleaner, a microwave oven, and kitchen appliances can give insights into a person’s current activities. Instead of putting a sensor on each appliance, our technique is based on the idea that appliance usage can be sensed by their manifestations in an environment’s existing electrical infrastructure. Prior approaches using this technique could only detect an appliance’s on-off states; that is, they only sense “what” is being used, but not “how” it is used. In this paper, we introduce DOSE, a significant advancement for inferring operating states of electronic devices from a single sensing point in a home. When an electronic device is in operation, it generates time-varying Electromagnetic Interference (EMI) based upon its operating states (e.g., vacuuming on a rug vs. hardwood floor). This EMI noise is coupled to the power line and can be picked up from a single sensing hardware attached to the wall outlet in a house. Unlike prior data-driven approaches, we employ domain knowledge of the device’s circuitry for semi-supervised model training to avoid tedious labeling process. We evaluated DOSE in a residential house for 2 months and found that operating states for 16 appliances could be estimated with an average accuracy of 93.8%. These fine-grained electrical characteristics affords rich feature sets of electrical events and have the potential to support various applications such as in-home activity inference, energy disaggregation and device failure detection.

## I. INTRODUCTION

The ability to sense, model, and infer human activity in the physical world remains an important challenge in pervasive computing. *Infrastructure-mediated sensing* has been proposed as one method for low-cost and unobtrusive sensing of human activities [2,6,7,14,15,16,22]. This technique is based on the idea that human activities (e.g., vacuuming, using the microwave, or blending a drink) can be sensed by their manifestations in an environment’s existing infrastructures (e.g., a home’s water, electrical, and HVAC infrastructures), thereby reducing the need for installing sensors everywhere in an environment. In one example of IMS, Patel *et al.* demonstrated the ability to detect electrical events using a single plug-in sensor by fingerprinting the transient electrical noise signatures on the power line [15]. Gupta *et al.* improved on this method by utilizing the electromagnetic interference (EMI) produced by modern electronic devices in the home [7]. From a single sensing point, the presence of electronic devices can be inferred by training on the frequency domain EMI signatures of those devices. Although useful, these techniques only detect the on/off state of electronic devices. However, the continuous time-varying EMI provides many more clues on

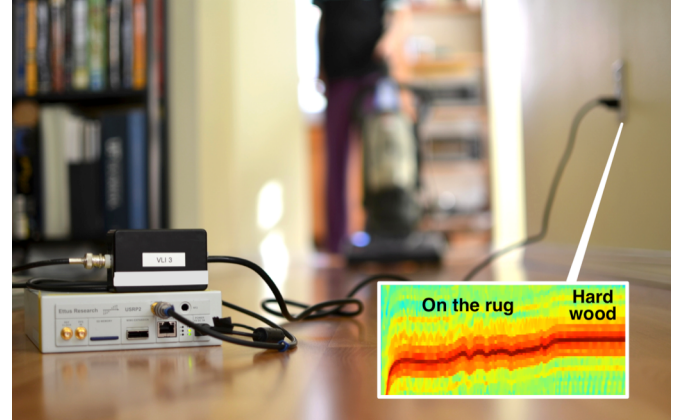


Figure 1: DOSE detects user-driven operating states of electronic appliances through a single sensing point installed anywhere in the house.

how a device is being used and what state the device might be in, providing more granular information for activity recognition and energy disaggregation.

To this end, we present a technique to detect the operating states of electronic devices through a single-sensing point which can be installed anywhere in the home (see Figure 1). DOSE (Detecting Operating States of Electronic devices) leverages electrical noises for estimating the operating states of appliances. Electronic devices yield electromagnetic interference (EMI) when they are in operation [7]. We found that when an electronic device operates at different states (e.g., high vs. low CPU loads) or under varying conditions (e.g., using vacuum cleaner on rug vs. hardwood floor), their EMI fluctuates distinctively based on the corresponding user behaviors. By analyzing time-varying EMI, we are able to identify various operating states of an electronic appliance. In particular, we leverage domain knowledge of the device’s circuit model and semi-supervised clustering for state estimation, obviating the need of tedious labeling process on the data. This usage of domain knowledge as a prior for model training, instead of data-driven approaches, can significantly reduce the training efforts as it does not require huge amount of labeled data. In contrast to [7] which focused on static, SMPS-based EMI for electrical event detection, we investigated *time-varying* EMI induced by mechanically switching (e.g., vacuum cleaner), electronically switching (e.g., laptop), and the combination (e.g., hair dryer) circuits.

Understanding and discovering the operating states of electronic appliances can be beneficial to a variety of applications. For instance, these fine-grained electrical characteristics are richer feature sets than static features used in [7] and could be employed to achieve accurate energy disaggregation. In addition, the state changes in electrical characteristics are indicative of human behaviors and could be used in activity-inference research. For example, two residents could use the hair dryer very differently. By detecting the operating states in their respective usage patterns, the system could identify energy usage attributed to different individuals. Finally, the system could also be used for machine failure discovery by observing changes in known states or detecting the presence of a new, abnormal operating state. Detecting the states, then, is a vital first step to realizing these applications.

Specifically, the contributions of this paper include:

- A novel, low-cost technique for sensing operating states of electronic devices using time-varying EMI from a single sensing point.
- An algorithm leveraging domain knowledge and using semi-supervised learning techniques to obviate the need of labeled data, which significantly reduces the training effort.
- An analysis showing high detection accuracy across 16 electronic appliances in a real home setting.

## II. RELATED WORK AND BACKGROUND

Detecting electrical events has been accomplished using distributed sensors – one sensor on each appliance [4,21]. Although this approach is straightforward, it requires costly installation process and maintenance, and does not reveal operating states of an appliance. While other camera-based approaches are effective to capture electrical events and avoid the need of installing disturbed sensors [12,24], it raises potential privacy issues in real home settings and therefore restricts its applicability. Our approach on the contrary does not require any visual input and can detect electrical events and its corresponding states using a single sensing hardware.

The alternative approach is NALM (Non-intrusive Appliance Load Monitoring), a single instrumentation inline with the power meter to collect total energy usage of a household [8]. This approach detects a step change in power consumption data for sensing disaggregated energy attributed to individual appliances [11,17,18]. Recent works further showed the aggregated energy data can reveal a variety of private information of a household such as occupancy [10], eating/sleeping routines [13] or habitual behaviors [1]. Although NALM is an effective tool for detecting electrical events, the above works relied on a step change in consumption data, which usually requires high-frequency consumption measurements [9] and intensive training process [23].

Alternatively, infrastructure-mediated sensing (IMS) detects the electrical activities through events that affects the house's utility infrastructure [2,6,7,14,15,16,22]. Prior IMS research by Patel *et al.* has shown transients by mechanical switches can be used for electrical event detection [15]. Taking a step further, Gupta *et al.* leveraged EMI (Electromagnetic

Interference) sensing to capture the electronic activations [7]. Most recent electronic devices employ switched-mode power supply (SMPS), which is highly efficient and compact in size, but unavoidably causes loud EMI noise. These noises can be regarded as the fingerprint of distinct devices and repurposed for electrical event detection. Similar EMI sensing technique was also shown in industrial applications for detecting motor failures [20].

Our approach is in spirit similar to ElectriSense [7]; however the goal and fundamental algorithm are quite different. ElectriSense was designed to detect on/off electrical events using static EMI caused by SMPS-based electronic appliances. DOSE, on the other hand, can detect an appliance's operating states using *time-varying* EMI caused by different sources, including mechanical switching, electronic switching and the combination circuit. Different from Gaussian fitting and supervised learning in [7], our algorithm leverages domain knowledge of the device's circuitry for semi-supervised learning, reducing efforts required in training the classifier.

## III. THEORY OF OPERATION

In this section, we detail the different types of time-varying EMI and how they vary with changes in the appliance's internal operating states or under different physical uses.

### A. EMI for Motor-based appliances

Motors exist in a variety of home appliances such as vacuum cleaners, blenders, and food mixers. Commutator motors (Figure 2) are energy efficient because they yield high rotational speed with relatively low power consumption. However, due to mechanical switching mechanism between the brushes and commutator, it inevitably generates strong EMI.

Figure 2 illustrates the schematic view of a three-slot, two-pole brushed motor. This motor consists of three commutator slots and three electromagnets, each of which has two poles (north and south). Two brushes are used to supply electric currents to the circuitry. When the motor is in operation (Figure 2, left), electric currents from commutators induce magnetic fields on iron bars, turning them into electromagnets (the "bars" insides the commutators in Figure 2). It is noted that the 3<sup>rd</sup> iron bar does not form any magnetic field as there is no current flowing through it. There are two permanent magnets on both sides to generate rotation forces. In this example, the 1<sup>st</sup> iron bar is attracted by the left permanent magnet while the 2<sup>nd</sup> is repelled, generating a clockwise force to the motor. The breaking and making of contacts between the commutator and brushes causes poles of the conducted electromagnets to switch, forcing the motor to consistently rotate clockwise (Figure 2, right). High-efficiency motors have more slots (usually 21 ~ 25) and even more brushes to yield a stronger torque.

*1) Commutating EMI due to mechanical switching:* The motor EMI is caused by the mechanical switching phenomena. As the motor rotates, the action of breaking and making contacts between the commutator and brushes yields periodic current spikes at the motor's rotation rate multiplied by the number of commutator slots. That is, the EMI appears at the

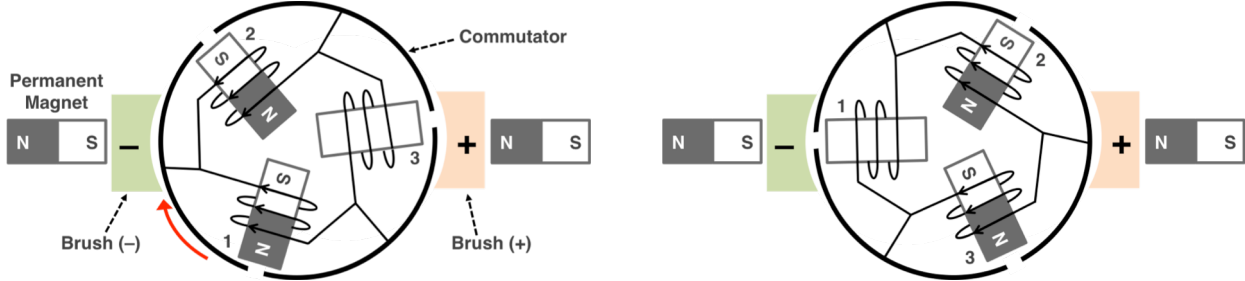


**Figure 2:** The schematic view of a three-slot, two-pole brushed motor. (*Left*) When the motor is on, electronic currents through commutators (arcs) turn iron bars into electromagnets, generating a clockwise force. (*Right*) Breaking and making contacts between commutators and brushes switches poles of conducted electromagnets, making the motor consistently rotate clockwise and generating EMI.

harmonics of the motor's rotation speed. For example, a motor with 21 slots and a rotation rate of 460 RPS (revolutions per second) yields current spikes at  $21 \times 460 = 9660$  Hz, which manifests itself as EMI of the same frequency. This type of EMI, called *commutating EMI*, propagates mainly through conduction over the powerline network and also yields a small amount of radiated emissions. When the motor is turned on, it takes one to two seconds to reach the specified operating speed. This speed-up duration appears as a “ramp-up” EMI (see Figure 3 and 4). In addition, there exists electrical resistance between each brush-commutator terminals. These impedances affect motor rotations, causing relatively weaker EMI near the fundamental frequency. We leverage these EMI as features for estimating motor operating states. We will detail our state detection algorithm in a later section.

2) *Time-varying EMI at different rotation speeds:* Commutating EMI appears at the harmonics of the motor's rotation rate. When the motor operates at a different speed, the EMI in turn appears at distinct frequencies. Figure 3 shows fluctuating EMI when a blender (Cuisinart PowerBlend600) operates at different speeds. In the first duration (5s ~ 10s in Figure 3), the blender was running at a relatively low speed, yielding EMI at roughly 6 kHz. When it switches to a higher speed (10s ~ 15s in Figure 3), EMI frequency ramps up to 7.1 kHz as the motor's rotation rate increases.

3) *Time-varying EMI in response to physical use:* It is noted that when the blender motor spins at a higher speed,

water within the blender container is vigorously stirred, causing air pockets and liquid to collide randomly with the blades. This uneven air/liquid resistance causes the blender speed to fluctuate, thus resulting in the irregular fluctuating EMI (as visible in Speed 4 section of Figure 3). We also observed time-varying EMIs when a vacuum is used on different surfaces. Figure 4 illustrates the fluctuating EMI when a vacuum cleaner (Bissel 6584) was used on the rug and hardwood floor. In a vacuum cleaner, the motor spins to exhaust the air from the machine, making the dust collection container a temporary vacuum. To balance the pressure, the air outside the cleaner flows into the container and then releases from the motor vent. This air circulation sucks the dusts into the machine and releases the air from the machine. When being used on the rug, the motor rotates at a lower, uneven speed due to the disturbed airflows by the rug. The reduction and disturbance in motor rotations therefore yield an EMI that fluctuates at a relatively low frequency (5s ~ 15s in Figure 4). Once the vacuum cleaner moves to a hardwood floor, the air intake becomes largely unhindered yielding static EMI at a higher frequency (16s ~ 21s in Figure 4).

#### B. EMI for SMPS-based appliances

SMPS (switched-mode power supply) has been extensively used in modern electronic appliances due to its small size and high efficiency. Unlike traditional linear power supply, SMPS manages power by switching the supply between complete-on,

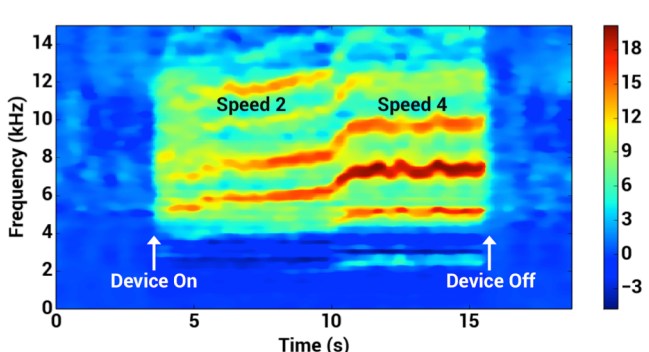


**Figure 3:** Time-varying EMI of a blender operating at different speeds. Higher rotation speed (from 10s to 15s) produces EMI at a higher frequency of 7.1 kHz.

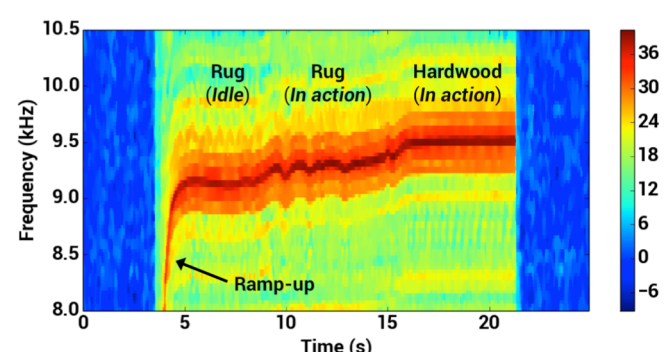


**Figure 4:** Time-varying EMI of a vacuum. When being used on a rug (from 5s to 15s), the motor rotates at lower speed and yields fluctuating EMI due to uneven airflows.

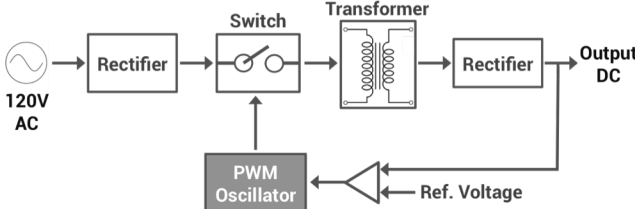


**Figure 5: Block diagram of an AC-to-DC SMPS.** Voltage regulation is accomplished by adjusting the ratio of on-off durations of PWM oscillator, which causes time-varying EMI in different operating states.

complete-off and low dissipation. Because the power supply operates at high dissipation only for a very short period, it minimizes unnecessary power wastage. Figure 5 shows the block diagram of an AC-to-DC SMPS. The key component of SMPS is a pass-transistor; it controls the frequency of oscillator that switches the stored energy from the inductors to the load that an electronic device requests. To reduce the size of the supply, SMPS usually operate from tens to hundreds of kilohertz. This switching action inherently generates strong EMI near the frequency where SMPS switches between different modes. We will refer this frequency as *switching frequency*. Gupta *et al.* leveraged SMPS-based EMI for electrical event detection and have shown the stability of signal patterns across different homes [7]. In DOSE, we take a step further and analyze time-varying EMI to discover operating states of SMPS-based appliances such as laptops and TVs.

1) *Time-varying EMI at different CPU loads:* In SMPS, output voltage regulation is accomplished by adjusting the ratio of on-off durations. As shown in Figure 5, the output DC is compared with the reference voltage to adjust switching frequency of the PWM (pulse-width modulation) oscillator. Electronic appliances with varying loads such as laptops can cause EMI fluctuations near its switching frequency. Figure 7 illustrates the time-varying EMI of a laptop (Acer Aspire 5736Z) with its CPUs operating at idle, medium and high load. When the CPU is running at a *high* load (i.e., 90~100%), the dropping output voltage causes the oscillator to operate at a higher frequency to draw more energy, yielding the EMI at higher frequency and magnitude (Figure 7, right). In other two modes, *idle* and *medium* load, we observed relatively weaker

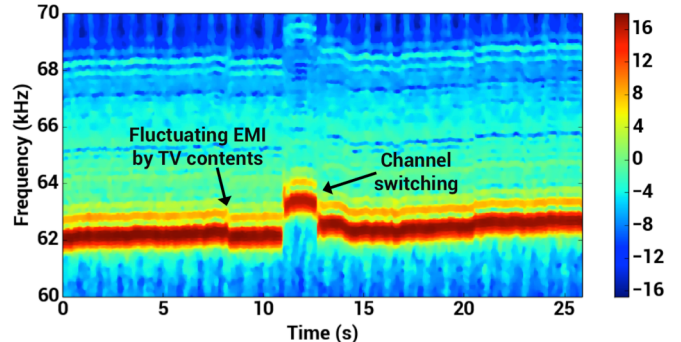


**Figure 6: Time-varying EMI of a TV.** When a TV is switched to another channel, the TV tuner resets the center frequency, resulting in a transient glitch (11s~13s) in its EMI signal.

but still discernible EMI (Figure 7, left and middle). We note that the signal patterns are distinct on different laptops and PCs that can be attributed to manufacturer differences in power regulation circuitry. These unique fingerprints between different computers could be used for manufacturer identification or abnormal detection, such as detecting large power draws that may indicate an impending device failure (e.g., a malfunctioning video card).

2) *Time-varying EMI caused by transient actions:* Another type of time-varying EMI that we observed is caused by transient actions such as switching a TV channel. Figure 6 shows the EMI signal of a TV (Sharp 42-inch) when it is switched from one channel to another. As shown in Figure 6, we observed a glitch, or sudden change in EMI, between 11s ~ 13s when the action was performed. On further investigation of the TV tuner's circuitry and operation, we found that when a TV switches to a new channel, the TV tuner resets the center frequency, causing the oscillator to operate at a different frequency for a short period. Prior research by Enev *et al.* has shown that TVs produce varying EMI signals that correlate to the screen content being displayed [3]. The EMI change from a channel switch is distinct from EMI change as a result of screen content; we have found that due to its large transient nature, it can be robustly detected and extracted.

### C. EMI for appliances with large resistive loads

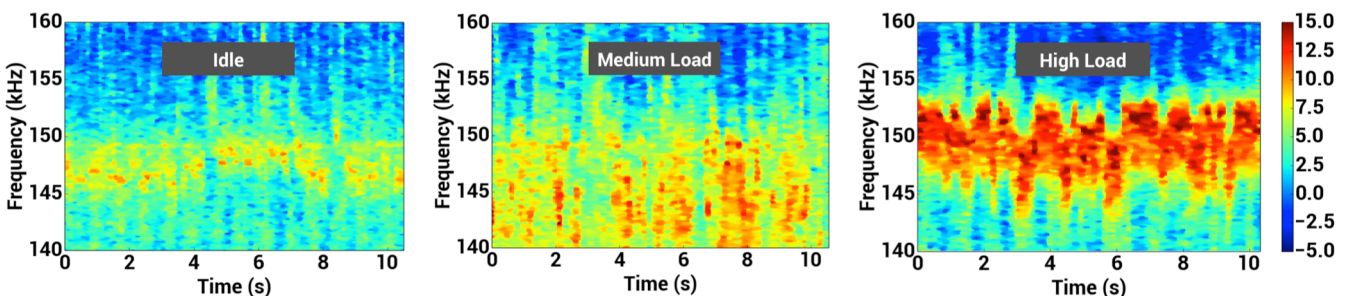


**Figure 7: Time-varying EMI of a laptop (Acer Aspire, 15-inch) with its CPU at idle (left), medium load (middle) and high load (right).** When the CPU is running at high load, the dropping output voltage causes the oscillator to operate at a higher frequency to draw more power, yielding the EMI at a higher frequency and magnitude.

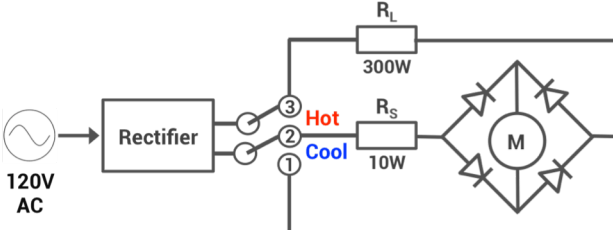


**Figure 8: The simplified schematic view of a dual-mode hair dryer.** While the device was switched to “hot” mode (i.e., terminal 2 and 3), a large, parallel resistance ( $R_L$ ) increases total current loads to the circuitry and affects rotation speed of the motor-driven fan (marked as “M”), causing time-varying EMI (example in Figure 9).

In addition to a motor, certain appliances such as hair dryers and fan heaters employ large resistive components to generate a stream of hot air. When the device is running in different modes (e.g., warm vs. hot), changes in resistive loads affect the motor operation and result in discernible EMI patterns for state estimation. Of course, this finding extends to other appliances where any other component affects motor operation as well, such as a torque screwdriver.

Figure 8 illustrates a simplified schematic view of a dual-mode hair dryer (i.e., generating hot and cool air). The AC source is first rectified to DC current. When the hair dryer operates at *cool* mode (i.e., making contacts at terminal 1 and 2 in Figure 8), only the low resistive load ( $R_S$ ) and the motor-driven fan are actuated. When it switches to *hot* mode (i.e., terminal 2 and 3 in Figure 8), the large resistive load ( $R_L$ ) is in parallel with  $R_S$ , which increases the total current load to the circuitry and changes the fan’s rotation speed. These behavior changes induce distinct EMI patterns at respective operating states. Figure 9 shows an example of this time-varying EMI when a hair dryer switches from the cool to hot mode.

#### IV. ALGORITHM

Figure 10 shows the processing pipeline for operating state detection and classification. We detail each component of our algorithm in this section.

##### A. Data Acquisition

To record EMI signals, we follow the experimental setup in [7] with minor adjustments. A power line interface (PLI) is plugged in the wall outlet to obtain the analog signal (see Figure 1). The PLI was modified from [7] and has a high-pass filter with cut-off frequency at 5.3 kHz. This corner frequency was chosen to strongly reject 60 Hz and harmonics, avoiding possible damages to the sensing hardware while being low

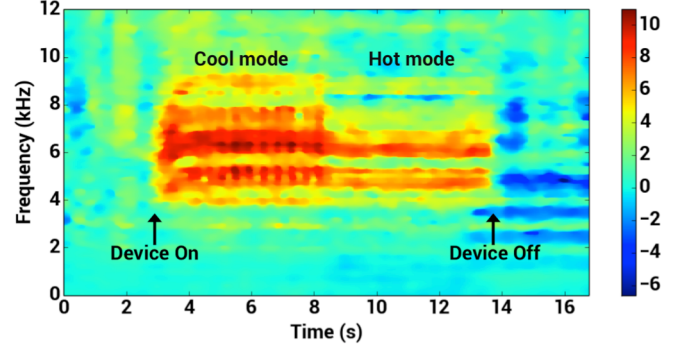


**Figure 9: Time-varying EMI of a hair dryer in two different operating temperatures.**

enough to capture low RPS motor EMI. The filtered signal is fed into a USRP (Universal Software Radio Peripheral) N210, which functions as an ADC (analog-to-digital) converter sampling at 500 kHz. We next compute Fast Fourier Transform (FFT) over these time-domain data, yielding 16384-point FFT vectors with 30.52 Hz bins. This resolution of bin size allows us to observe small EMI fluctuations in different operating states. The FFT vectors are streamed to our processing pipeline for state detection and classification.

##### B. Pre-processing

We first remove the baseline signal from recorded data. To this end, we average the first 100 FFT vectors in each recorded data file as the baseline vector, and subtract it from the remaining FFT vectors. The differential vectors represent EMI produced by a later-actuated electronic device. Next we perform filtering to remove noises resulting from the sensing hardware and powerline network. In particular, we apply a median filter with a window size of 10 to removed sparse noise. To further smooth the data, we use TVD (Total Variation Denoising) with regularization parameter of 20 [19]. TVD was designed to remove noise from images with high total variation while preserving important details such as corners and edges. Since EMI signals inherently have excessive, sparse noises, TVD can efficiently remove the noise without damaging most signal characteristics.

##### C. Event Detection

After the noise and baseline removal, we truncate the recorded data to extract the event segments. In particular, we sum up each FFT vectors and plot the total magnitude fluctuation over time (Figure 11, top). Any significant variation in this curve represents a possible electrical event and can be easily segmented by a threshold-based approach. Figure 11 demonstrates this event detection procedure. The top figure in

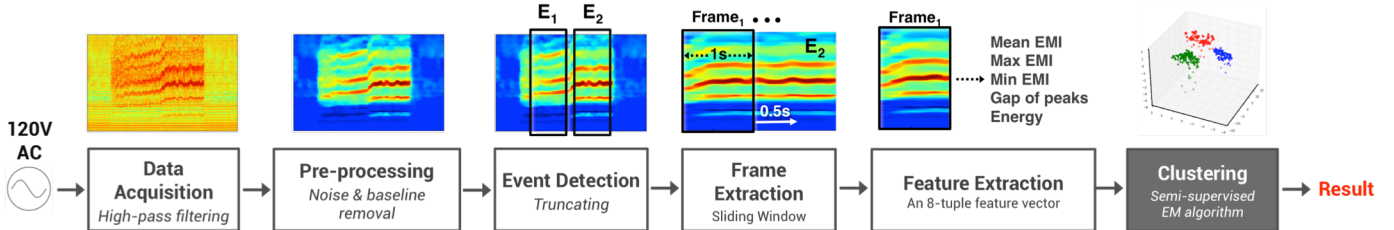


**Figure 10: Processing pipeline of operating state detection and classification.**

Figure 11 shows the normalized magnitude of the EMI data, where the rising and falling edge respectively correspond to *on* and *off* of an electrical event. To identify the event, we take the 1<sup>st</sup> derivative of this magnitude curve (Figure 11, bottom). The intersection of the threshold lines (dotted lines) and the 1<sup>st</sup> derivative curve denotes the start and end of an event (red circles). In this study, we empirically decided the threshold value of 0.0025 using the data collected from our study. This threshold is able to robustly detect all electrical events while inducing only two false alarms.

After extracting the event segment, we further truncate the FFT vectors to a specified frequency range that covers all operating states of a device. This 2<sup>nd</sup> truncating procedure is critical for the feature extraction. As we will only extract features within the specified spectrum, the truncated FFT vectors can more precisely represent the signal characteristics. Previous research [7] has shown that the target EMI frequency can be easily located by switching a device on and off, and therefore, we assume such information already exists. In this study, we manually turn on and off for each operating state of a device to retrieve the target frequency range of each device.

#### D. Frame Extraction

For the truncated event segment, we further chunk into smaller units (called *frames*) by a sliding window of 1 second with 0.5s overlapping. According to our observations, the EMI shows stable signal characteristics within the same operating state. This short-term analysis therefore serves two purposes in this study: (1) to confirm the stability of EMI characteristics within the same operating states, and (2) if EMI fluctuates dramatically in the same states, to analyze the variation.

#### E. Feature Extraction

We extract aggregated features from each frame based on signatures of different time-varying EMI. The first six features are *mean*, *max* and *min* magnitude and frequency of the peak EMI of the frame; they describe the characteristics of the fundamental EMI. For motor-based devices, there usually exist multiple peak EMIs due to uneven rotations caused by the fractions and electric resistance. To capture this, we extract the frequency *gap* between two dominant EMI peaks as the 7<sup>th</sup> feature. Some EMI has distinct total magnitude variation such as laptop (under different CPU loads) or hair dryer (under different temperature modes). Therefore we choose *mean magnitude* of the frame as the 8<sup>th</sup> feature. In the end, the system extracts an 8-tuple feature vector for each frame.

#### F. Clustering

For classification of operating states, we choose EM (expectation maximization) clustering algorithm due to some key advantages. One advantage of the EM algorithm is its adaption to uneven cluster sizes. As we expect a resident may use each device in different states unevenly in daily life, thus the cluster sizes corresponding to different states may vary a lot. EM typically outperforms other similar algorithms such as k-means which is more sensitive to the cluster size. In addition, EM allows clusters to overlap. If an appliance has two similar operating states (e.g., similar rotation speed in 2 modes of a food mixer), their respective clusters will unavoidably overlap in the feature space.

Perhaps more importantly, EM only requires the number of clusters as the input parameter. From the user perspective, we perceive the states of an appliance either from its *outlook* (e.g., 6 buttons of a blender), *physical use* (e.g., vacuuming on different surfaces) or its *circuitry model*. Whenever we get a new device, this human observation can be employed as a prior knowledge to train the model, obviating the need to label each individual state during calibration. We leverage this domain knowledge to determine the input parameter (i.e., the number of clusters) to our EM classifier. In this prototype, we applied EM clustering on individual appliances and trained their models separately. For implementation, we used Scikit-learn package, a machine learning library for Python.

## V. EVALUATION, RESULTS AND ANALYSIS

### A. Study Design

We set up our experiments in a real home environment. This residential house is a triplex, 1100 sq. ft. townhouse of two residents (one male, one female). To explore the temporal stability of the signal, the data collection process was conducted across 2 months, including multiple sessions at different time (morning, afternoon and night) on both weekdays and weekend. During each session, we asked one resident to turn on a device to a specified operating state for a random time (5s ~ 10s) and then turned it off. When one resident was executing the requested action, the other resident remained performing her daily routines such as cooking, using computers or watching TV. Each electrical event was manually labeled. It is noted that these labels are only used for evaluation, not for model training. Throughout the study, 580 electrical events were collected in total.

To collect the data, we installed the sensing hardware (i.e., a PLI and USPR N210) and a laptop in the participant's house. The laptop is a local server for recording EMI data and the follow-up processing pipeline. For each type of time-varying EMI, we respectively chose four to six different appliances and in total, 16 electronic devices were evaluated in our study. Table I shows the list of these devices. As ElectriSense [7] has shown the stability of EMI signals across different homes, we believe findings in this study can apply to other households.

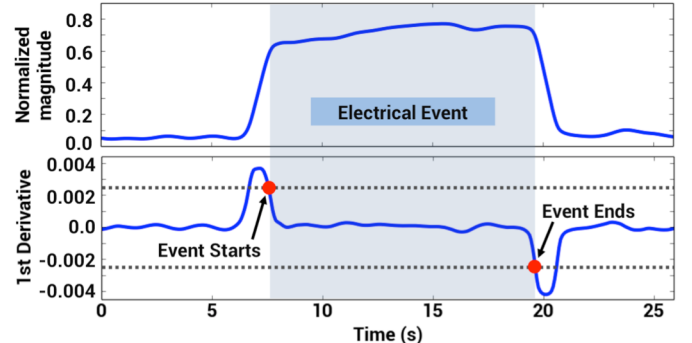


**Figure 11: Event detection procedure. (Top)** Rising and falling edges represent on/off of an electrical event. **(Bottom)** The intersection of the threshold lines (dotted) and 1<sup>st</sup> derivative curve of the top curve represents the start and end of an electrical event (red circles).

TABLE I. THE LIST OF DEVICES IN OUR STUDY AND CLASSIFICATION ACCURACY.

EMI type	Device	Make / Model	Operating states	Actual clusters	Predicted clusters	Accuracy
<b>Motor-based</b>	Vacuum Cleaner	Bissel 6584	Rug / Hardwood / Hose	3	3	<b>100%</b>
		Hoover Elite II		3	3	<b>100%</b>
		Eureka 1432A		2	2	<b>98.5%</b>
	Blender / Food mixer	Hamilton Beach 62560		6	5	<b>87.4%</b>
		Cuisinart PowerBlend 600	6 Rotation Speed	6	6	<b>89.9%</b>
		Oster Listed 654A		6	6	<b>84.0%</b>
<b>SMPS-based</b>	Laptop / Computer	Acer Aspire 15"	Idle / Medium / High Load	3	3	<b>99.7%</b>
		Dell Inspiron 15"		3	3	<b>98.8%</b>
		Toshiba Portege 13"		3	3	<b>92.1%</b>
		PC (300W)		3	3	<b>100%</b>
	Television	Vizio 32"		*	*	<b>100%</b>
		Sharp 42"	Channel switching (hit rate)	*	*	<b>90%</b>
<b>Mixed</b>	Hair Dryer	Remington Speed2Dry	Cold / Warm / Hot	3	3	<b>81.5%</b>
		Tashin Powerslit TS-318A		3	3	<b>81.8%</b>
		Tashin TS-3000		3	3	<b>96.7%</b>
		Gibson GSN-760		3	3	<b>100%</b>

### B. Defining Operating States

Different appliances of the same type usually have minor difference in operating states. For example, one blender has 6 speed modes while the other may have 7. In this study, we chose the same number of states for devices within the same categories in order to get a baseline to compare between them (see *Operating states* Table I).

1) *Operating states of motor-based devices*: For vacuum cleaners, we defined two states based on the surface where it is used (i.e., on a rug or hardwood floor). Most vacuum cleaners have a hose, which can be detached from the machine and used separately. Here we defined “using the hose” as the 3<sup>rd</sup> state. One of our vacuum cleaners (Eureka 1432A) does not equip a hose so we only evaluated it on two defined surfaces. For other motor-based appliances (i.e., blenders and food mixer), the states are defined as their operating speeds.

2) *Operating states of SMPS-based devices*: For laptops, we defined three different states based on CPU loads. In the idle mode, we turned off all applications and keep the CPU load below 10% usage. In the medium load, we run our testing script that periodically calculates a specified math equation and meanwhile open a couple webpage and youtube videos, maintaining CPU loads floating between 30% and 60%. To simulate a high load, we run an online benchmark called SilverBench<sup>1</sup>, forcing CPU usage above 90%. For TV, we define the state as the action of switching a channel.

3) *Operating states of mixed-mode devices*: We defined states of a hair dryer by the operating temperatures – cold, warm and hot. Some modern hair dryers have various temperatures modes combining with different fan speeds. As the factor of speed has been evaluated in motor-based appliances (i.e., vacuum cleaner, blender and food mixer), in

this category, we focus on temperature variation, that is, how a large resistive load affects the time-varying EMI.

### C. System Performance and Analysis

As EM is semi-supervised learning, the output of our processing pipeline are unlabeled clusters, each of which represents an unknown operating state. For analysis purposes, we assigned each predicted cluster to its actual class based on majority vote using labels that were annotated in our data collection process. Clusters with the same voting results are merged. Table I shows the classification results of individual appliances.

Overall our system presents the average accuracy of 93.8% across 16 appliances. All vacuum cleaners report high classification accuracy. We noted that the 3<sup>rd</sup> state (i.e., using the hose) shows a highly discernible cluster in our trained EM model. In the study, we asked the participant to use hose to clean the corner of a wall. Compared to the machine used on a rug, the hose moves unevenly above the surface and causes an irregular EMI fluctuation. In addition, the detachment of a hose affects the airflows through the container due to changes in air pressure. These two factors causes time-varying EMI distinct from the other two modes (i.e., rug and hardwood floor), yielding high classification accuracy.

Similarly, almost all laptops/PC and TV report high accuracy. Toshiba laptop (13") reports a slightly lower accuracy (92.1%). As this model produces weaker EMI than other computers, it induces less discernible EMI between different CPU loads; the confusion occurs between the “idle” mode (recall=81.7%) and “medium load”. The EMI of Sharp TV (42") is sensitive to the contents being displayed and produced some dramatically fluctuating EMI. In such case, the EMI caused by channel switching becomes unrecognizable and thereby slightly downgrades the event detection rate (hit rate of 90%). To further explore the system robustness, we recorded 40-min EMI data from both TVs without any actions of

<sup>1</sup> SilverBench: <http://silver.urih.com>

channel switching. We only detected two false alarms, showing the robustness of our algorithm against this fluctuation.

Blenders and food mixers show a relatively low accuracy (84% ~ 89.9%). The Hamilton food mixer has confusions between speed mode 2 and 3, which are merged into the same class with low accuracy (recall=54.7%). Similarly, the Cuisinart blender has confusions between speed mode 3 and 4 (recall=64.4%), while the Oster blender exists confusions among speed mode 1 (recall=76.5%), 2 (recall=65.9%) and 3. These confusions are resulted from the similar characteristics between operating states. When we examined the data, we found frequency and magnitude of the confused states are quite similar. After filtering (Figure 10, the 2<sup>nd</sup> step), these minor differences between states are smoothed out and become hard to differentiate. It implies that fundamentally the device does not have as many *discernible* operating speeds as it claims.

Finally, we saw high variations in accuracy of hair dryers (81.5% ~ 100%). For two hair dryers with relatively low accuracy (81.5% and 81.8%), the confusion occurs between the “cold” and “warm” mode. We observed similarly EMIs in these two modes. Our inference is that in the warm mode, the parallel resistive load is small in these devices. That is, it does not cause discernible changes in the total current loads compared to that in cold mode, yielding similar EMI patterns. As described earlier, the difference in circuit design between hair dryers is attributed to different manufacturers.

## VI. DISCUSSION AND FUTURE WORK

### A. Energy Disaggregation

In this work, we showed distinct signal characteristics when a device operates at different operating states. For the same type of devices, we further found that there also exist minor differences in their EMI. For example in the Oster blender (Listed 564A), we observed a strong EMI between its fundamental and 1<sup>st</sup> harmonic, while we did not see similar pattern in other blender or food mixer. Gibson hair dryer (GSN-760), instead of a continuous EMI, produces a switching-style EMI when operating at cold mode. Similarly in Vizio 32” TV, when switching to a new channel, the TV produces a transient, scanning-style EMI between 115 ~ 145 kHz (see Figure 12). This transient signal in spectrum is away from its fundamental frequency and was not found on the other TV. These small but significant differences between devices could provide granular information for manufacturer

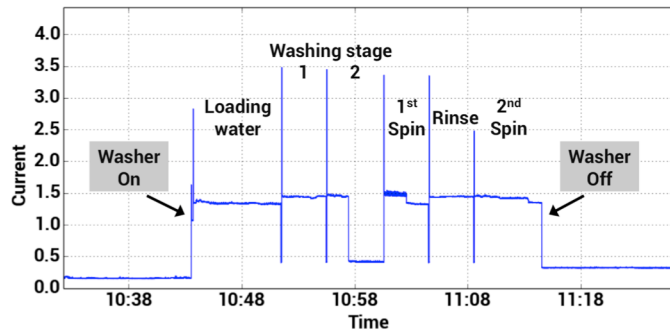


**Figure 13: Current loads of a stacked washer, showing discernible patterns that represent different stages.**

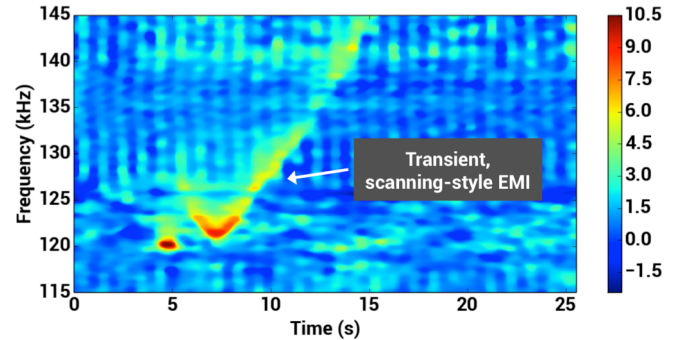


**Figure 12: Time-varying EMI of a TV. This TV produced a scanning-style EMI when it switches the channel.**

identification and energy disaggregation. Especially for same type of devices, their EMI usually overlap at similar frequency range (e.g., motor-based devices below 20 kHz). These nuance in time-vary EMI can be employed to differentiate them.

### B. Activity Recognition

Understanding fine-grained electricity data could be beneficial to activity-inference researches. For example, different behaviors of using a hair dryer (e.g., cold vs. hot) could imply different residents within a household. The duration of using the vacuum cleaner in different areas (e.g., rug vs. hardwood floor) could infer active areas in home. In addition, the fluctuating EMI of a blender could attribute to what food is being processed; for example, the action of “ice crush” shows time-varying EMI during the process. Finally, the action of switching a TV channel can be strongly indicative of a “watching TV” activity. This interaction between a resident and a TV might be difficult to capture through a motion sensor [12] as a sensor event does not directly related to the actual activity; it can be fired by other possible activities such as “reading”, “using a computer” or a pet passing through. We believe the finding in this work is the first step to support whole-home activity recognition.

### C. Combining Other Sensing Approaches

While we leverage time-varying EMI for operating states estimation, some home appliances such as old washer or fridge do not produce observable EMI signals. From an earlier survey by Froehlich *et al.*, the on/off states of these devices could possibly be extracted from their current or consumption data [5]. To collect the aggregated energy usage, we installed the experimental sensor provided by Belkin<sup>3</sup> in the participant’s house. Figure 13 shows the current loads of a stacked washer (General Electric, WSM-2420) in a complete high-load washing cycle. The current draws show discernible signal patterns in different operating states. Similar varying current draws can also be observed on a dishwasher (Whirlpool DU810SWP), as shown in Figure 14. To truly support the whole home activity inference, we believe it requires leveraging both time-vary EMI and disaggregated current/power data as we reported in this work. As described

<sup>3</sup> Belkin Echo Unit: <http://www.belkinbusiness.com/echo-water-0>

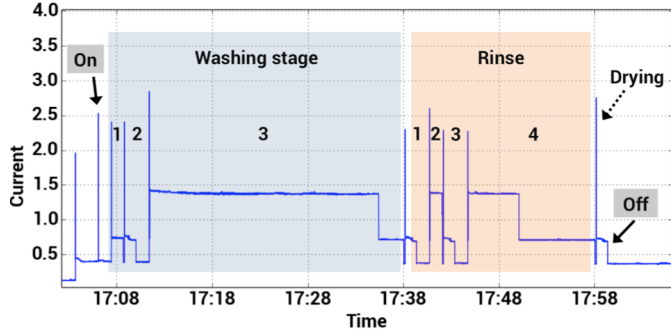


**Figure 14: Current loads of a dishwasher. The dishwasher was manually turned off after the drying stage began.**

earlier, disaggregating current or power usage from the total consumption relies on step changes in its signal. It requires further signal processing and machine learning technology to detect these step changes that attribute to different operating states. We leave it as the future work.

#### D. Detecting Machine Failure

The proposed system could also be applied for machine failure detection by observing changes in known states or the presence of a new, abnormal operating state. For example, a blender may show abnormal EMI caused by malfunction in its motor (e.g., observing EMI at a lower frequency when running at a relatively higher speed). A computer with high magnitude EMI in its idle mode may relate to a flawed hardware (e.g., a video card). A vacuum with a decreased frequency EMI could correspond to a plugged vent filter or even the motor failure. In the future, we will further explore these applications.

## VII. CONCLUSION

In this work, we demonstrate a sensing technique for detecting operating states of electronic appliances. Our approach utilizes time-varying EMI signal produced by electronic appliances when they are operating at different states. This EMI is coupled onto the power lines and can be captured using a single sensing hardware installed from anywhere in the house. Our algorithm used semi-supervised learning for state estimation, which exploits domain knowledge of the devices to train the classifier and avoids the need of manually labeled data. We show robust state estimation of our system through a 16-device study in a real home setting. DOSE affords a low-cost, single-point sensing approach to discover fine-grained features of electrical events for supporting applications such as energy disaggregation, machine failure detection or activity inference, in a smart home environment.

## REFERENCES

- [1] Abreu, J.M., Pereira, F.C., and Ferrao, P. Using pattern recognition to identify habitual behavior in residential electricity consumption. In *Proc. of Energy and Buildings'12*, pp. 479–487.
- [2] Cohn, G., Gupta, S., Froehlich, J., Larson, E., and Patel, S.N. GasSense: Appliance-Level, Single-Point Sensing of Gas Activity in the Home. In *Proc. of Pervasive'10*, pp. 265–282.
- [3] Enev, M., Gupta, S., Kohno, T., and Patel, S.N. Televisions, video privacy, and powerline electromagnetic interference. In *Proc. of CCS'11*, pp. 537–550.
- [4] Fishkin, K.P., Kautz, H., Patterson, D., Perkowitz, M., and Philipose, M. Guide: Towards Understanding Daily Life via Auto-Identification and Statistical Analysis. In *Proc. of UbiHealth'03*.
- [5] Froehlich, J., Larson, E., Gupta, S., Cohn, G., Reynolds, M., and Patel, S. Disaggregated End-Use Energy Sensing for the Smart Grid. *IEEE Pervasive Computing* 10, 1 (2011), pp. 28–39.
- [6] Froehlich, J.E., Larson, E., Campbell, T., Haggerty, C., Fogarty, J., and Patel, S.N. HydroSense: Infrastructure-mediated Single-point Sensing of Whole-home Water Activity. In *Proc. of UbiComp'09*, pp. 235–244.
- [7] Gupta, S., Reynolds, M.S., and Patel, S.N. ElectriSense: Single-Point Sensing Using EMI for Electrical Event Detection and Classification in the Home. In *Proc. of UbiComp'10*, pp. 139–148.
- [8] Hart, G.W. Nonintrusive appliance load monitoring. In *Proc. of the IEEE* 80, 12 (1992), pp. 1870–1891.
- [9] Kim, H., Marwah, M., Arlitt, M., Lyon, G., and Han, J. Unsupervised Disaggregation of Low Frequency Power Measurements. In *Proc. of SDM'10*, pp. 747–758.
- [10] Kleiminger, W., Staake, T., and Santini, S. Occupancy Detection from Electricity Consumption Data. In *Proc. of BuildSys'13*, pp. 1–8.
- [11] Liang, J., Ng, S.K.K., Kendall, G., and Cheng, J.W.M. Load Signature Study&#x2014;Part I: Basic Concept, Structure, and Methodology. *IEEE Transactions on Power Delivery* 25, 2 (2010), pp. 551–560.
- [12] Logan, B., Healey, J., Philipose, M., Tapia, E.M., and Intille, S. A long-term evaluation of sensing modalities for activity recognition. In *Proc. of UbiComp'07*, pp. 483–500.
- [13] Molina-Markham, A., Shenoy, P., Fu, K., Cecchet, E., and Irwin, D. Private memoirs of a smart meter. In *Proc. of BuildSys'10*, pp. 61–66.
- [14] Patel, S.N., Reynolds, M.S., and Abowd, G.D. Detecting Human Movement by Differential Air Pressure Sensing in HVAC System Ductwork: An Exploration in Infrastructure Mediated Sensing. In *Proc. of Pervasive'08*, pp. 1–18.
- [15] Patel, S.N., Robertson, T., Kientz, J.A., Reynolds, M.S., and Abowd, G.D. At the flick of a switch: detecting and classifying unique electrical events on the residential power line. In *Proc. of UbiComp'07*, pp. 271–288.
- [16] Patel, S.N., Truong, K.N., and Abowd, G.D. PowerLine Positioning: A Practical Sub-Room-Level Indoor Location System for Domestic Use. In *Proc. of UbiComp'06*, pp. 441–458.
- [17] Perez, M.N.V. A non-intrusive appliance load monitoring system for identifying kitchen activities. *Master Thesis*, 2011.
- [18] Reinhardt, A., Baumann, P., Burgstahler, D., et al. On the accuracy of appliance identification based on distributed load metering data. In *Proc. of SustainIT'12*, pp. 1–9.
- [19] Rudin, L.I., Osher, S., and Fatemi, E. Nonlinear total variation based noise removal algorithms. *Physica D* 60, 1–4 (1992), pp. 259–268.
- [20] Silva, A.M.D. Induction Motor Fault Diagnostic and Monitoring Methods. *Master Thesis*, 2006.
- [21] Tapia, E.M., Intille, S.S., and Larson, K. Activity Recognition in the Home Using Simple and Ubiquitous Sensors. In *Proc. of Pervasive'04*, pp. 158–175.
- [22] Thomaz, E., Bettadapura, V., Rayes, G., et al. Recognizing water-based activities in the home through infrastructure-mediated sensing. In *Proc. of UbiComp'12*, pp. 85–94.
- [23] Zeifman, M. and Roth, K. Nonintrusive appliance load monitoring: Review and outlook. *IEEE Transactions on Consumer Electronics* 57, 1 (2011), pp. 76–84.
- [24] Zouba, N., Boulay, B., Bremond, F., and Thonnat, M. Monitoring Activities of Daily Living (ADLs) of Elderly Based on 3D Key Human Postures. In *Proc. of ICVW'08*, pp. 37–50.